

1
2
3
4
5
6
7
8
9
10
11
12
13
14
15
16
17
18
19
20
21
22
23
24
25
26
27
28
29
30
31
32
33
34
35
36
37
38

Forecasting Wind Power Quantiles Using Conditional Kernel Estimation

James W. Taylor^{*a}

Saïd Business School, University of Oxford

Jooyoung Jeon^b

School of Management, University of Bath

Renewable Energy, 2015, Vol. 80, pp. 370-379.

^a Corresponding author. Saïd Business School, University of Oxford, Park End Street, Oxford, OX1 1HP, UK

Email: james.taylor@sbs.ox.ac.uk

^b School of Management, University of Bath, Bath, BA2 7AY, UK

Email: j.jeon@bath.ac.uk

39 **Abstract**

40 The efficient management of wind farms and electricity systems benefit greatly from accurate
41 wind power quantile forecasts. For example, when a wind power producer offers power to the
42 market for a future period, the optimal bid is a quantile of the wind power density. An
43 approach based on conditional kernel density (CKD) estimation has previously been used to
44 produce wind power density forecasts. The approach is appealing because: it makes no
45 distributional assumption for wind power; it captures the uncertainty in forecasts of wind
46 velocity; it imposes no assumption for the relationship between wind power and wind
47 velocity; and it allows more weight to be put on more recent observations. In this paper, we
48 adapt this approach. As we do not require an estimate of the entire wind power density, our
49 new proposal is to optimise the CKD-based approach specifically towards estimation of the
50 desired quantile, using the quantile regression objective function. Using data from three
51 European wind farms, we obtained encouraging results for this new approach. We also
52 achieved good results with a previously proposed method of constructing a wind power
53 quantile as the sum of a point forecast and a forecast error quantile estimated using quantile
54 regression.

55

56 *Keywords:* Wind power; Quantiles; Conditional kernel estimation; Quantile regression

57

58

59

60

61

62

63

64

65 **1. Introduction**

66 For many countries, the proportion of electricity consumption generated from
67 renewable sources is rapidly increasing, with ambitious targets aimed at reducing carbon
68 emissions. Wind power generation is a prominent feature of this development in sustainable
69 energy. The high variability and low predictability of the wind present a significant challenge
70 for its integration into electricity power systems [1]. An accurate estimate of the uncertainty
71 in the predicted power output from a wind farm is important for the efficient operation of a
72 wind farm, and indeed for the efficient management of a power system [2]. A common
73 purpose of wind power forecasting is to set the bid for sales of future production that a wind
74 power producer will make to an energy market. Pinson et al. [3] show that if, as is likely to be
75 the case, the unit cost of surplus and shortage wind power production are different, the
76 optimal bid is not the expectation of future production, but it is instead a quantile. It is,
77 therefore, a prediction of the quantile that is needed, and not a point forecast. The forecasting
78 of wind power quantiles is the focus of this paper.

79 One possible approach to wind power forecasting is to fit a univariate time series
80 model to wind power time series (e.g. [4]). However, this is very challenging due to the
81 bounded and discontinuous nature of wind power time series. It is more straightforward to fit
82 a time series model to wind speed and direction data, converted to Cartesian coordinates to
83 represent wind velocity variables (e.g. [5]). Forecasts of these variables can then be used as
84 the basis for wind power prediction. This is the approach taken by Jeon and Taylor [6] who
85 use conditional kernel density (CKD) estimation to produce a forecast of the wind power
86 probability density function (i.e. a density forecast). Their methodology incorporates (a) wind
87 speed and direction forecast uncertainty, and (b) the stochastic nature of the dependency of
88 wind power on wind speed and direction. We are not aware of other wind power density
89 forecasting methods that aim to capture these two fundamental sources of uncertainty. The
90 method would, therefore, seem to have strong potential. Although the resultant wind power

91 density forecasts can be used to provide quantile forecasts, it is our assertion in this paper that
92 superior quantile forecasts can be produced by an adaptation of this CKD-based
93 methodology.

94 Jeon and Taylor [6] optimise method parameters using an objective function that
95 measures density forecast accuracy. In this paper, we replace this by the objective function of
96 quantile regression, and hence calibrate the approach towards estimation of a particular
97 quantile of interest. The result of this is that the parameters are able to differ across the
98 different quantiles. This is appealing, because different quantiles are likely to have different
99 features and dynamics. For example, the left tail of the wind power distribution may evolve at
100 a faster rate than the right tail.

101 In this paper, we focus on hourly data from three European wind farms, and we
102 forecast wind power quantiles for lead times ranging from 1 hour up to 3 days ahead. Foley et
103 al. [7] describe how such short lead times are important for power system operational
104 planning and electricity trading. We base the estimation on density forecasts for wind speed
105 and direction, produced by a time series model. It is worth noting that these wind speed and
106 direction density forecasts can be replaced by ensemble predictions from an atmospheric
107 model [8,9,10]. We use density forecasts from a time series model, because this approach has
108 appeal in terms of cost, and the forecasts are likely to compare well with predictions from
109 atmospheric models for short lead times [11]. Also, by contrast with ensemble predictions,
110 time series model predictions can be conveniently produced from any forecast origin, for any
111 lead time, and for any wind farm location for which a history of observations is available.

112 As we have explained, our proposal is to use the quantile regression objective
113 function within a CKD-based approach. It is worth noting that quantile regression has
114 previously been used for wind power quantile prediction. Bremnes [12] proposes forms of
115 locally weighted quantile regression with wind speed and direction as explanatory variables.
116 The adaptive quantile regression procedure of Møller et al. [13], and the linear model with

117 spline basis functions of Nielsen et al. [14], involve the application of quantile regression to
118 the errors of wind power point forecasts produced in a separate procedure. As in the study of
119 Taylor and Bunn [15], Nielsen et al. simultaneously estimate quantiles for a range of lead
120 times by using the forecast error from different lead times as dependent variable, and by
121 using the forecast lead time as one of the explanatory variables. In a study of ramp
122 forecasting, Bossavy et al. [16] use quantile regression based on point forecasts of wind
123 power, speed and direction, as well as information on the magnitude and timing of the most
124 recent ramp. In this paper, we implement a form of the Nielsen et al. approach, and compare
125 quantile forecast accuracy with our proposed adaptation of the CKD-based approach of Jeon
126 and Taylor [6]. The CKD-based approaches explicitly try to capture the uncertainties
127 underlying wind power, while the quantile regression method is a pragmatic approach. It is an
128 interesting empirical question as to which is more accurate, and we address this in this paper.

129 Section 2 discusses the features of wind power, speed and direction data from three
130 wind farms. Section 3 reviews CKD-based wind power density forecasting, and Section 4
131 describes how the method can be adapted for the prediction of a particular quantile. Section 5
132 provides an empirical evaluation of the accuracy of our proposed CKD-based quantile
133 forecasting approach, and a quantile regression model based on the approach of Nielsen et al.
134 Section 6 provides a brief summary and conclusion.

135

136 **2. Wind data and the power curve**

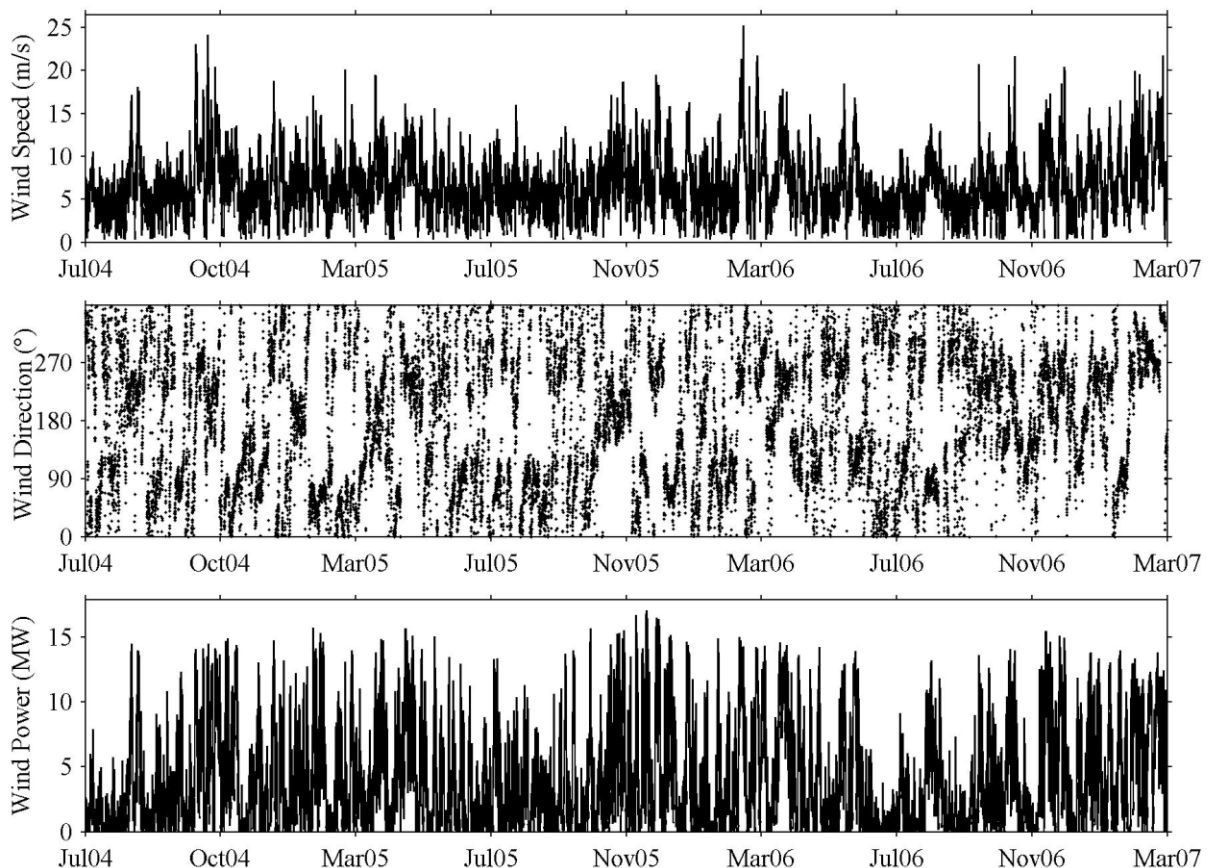
137 *2.1. The characteristics of wind data*

138 The data used in this paper consists of hourly observations for wind speed, direction
139 and power, recorded at the following three wind farms: Sotavento, which is in Galicia in
140 Spain, and Rokas and Aeolos, which are on the Greek island of Crete. Our data for Sotavento
141 is for the 23,616 hourly periods from 1 July 2004 to 11 March 2007. For Rokas and Aeolos,
142 the data is for the 8,760 hourly observations from the year 2006. The wind power data

143 corresponds to the total power generated from the whole wind farm. On the final day of each
144 dataset, the capacities of Sotavento, Rokas and Aeolos were 17.6 MW, 16.3 MW and 11.6
145 MW, respectively. The data from the two Crete wind farms was used in [6].

146 Fig. 1 presents the wind speed, direction and power time series for the Sotavento wind
147 farm. The series exhibit substantial volatility, which suggests that point forecasting is likely
148 to be very challenging, and this motivates the development of methods for quantile and
149 density forecasting. The plots also suggest that fluctuations in wind power coincide, to some
150 extent, with variations in wind speed and direction. It is interesting to note that the volatility
151 in the series varies over time. It is this that has prompted the use of generalised autoregressive
152 conditional heteroskedastic (GARCH) models for wind speed data (e.g. [5,9,17]). Fitting such
153 models to wind power time series is not appealing, because the power output from a wind
154 farm is bounded above by its capacity, and this creates discontinuities, as well as
155 distributional properties that are non-Gaussian and time-varying.

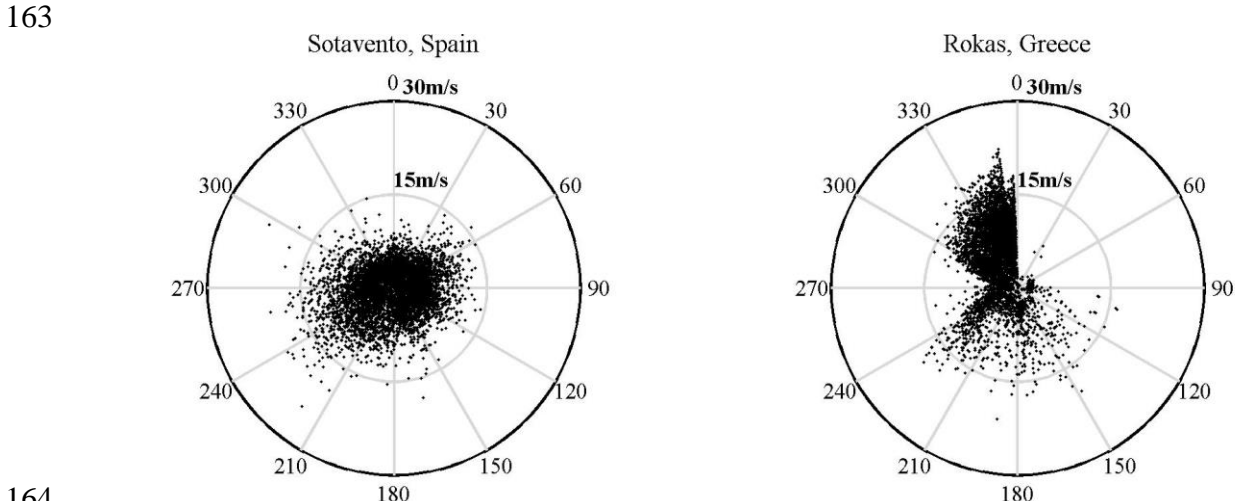
156



157

159 **Fig. 1.** Wind speed, direction and power time series for Sotavento.

160 For Sotavento and Rokas, Fig. 2 shows Cartesian plots of wind speed and direction,
161 where the distance of each observation from the origin represents the wind speed. The plot
162 for Rokas shows that north-westerly wind is particularly common at this wind farm.



164 **Fig. 2.** For Sotavento and Rokas, Cartesian plots of wind speed and direction, where the
165 distance of each observation from the origin is the strength of the wind speed.
166

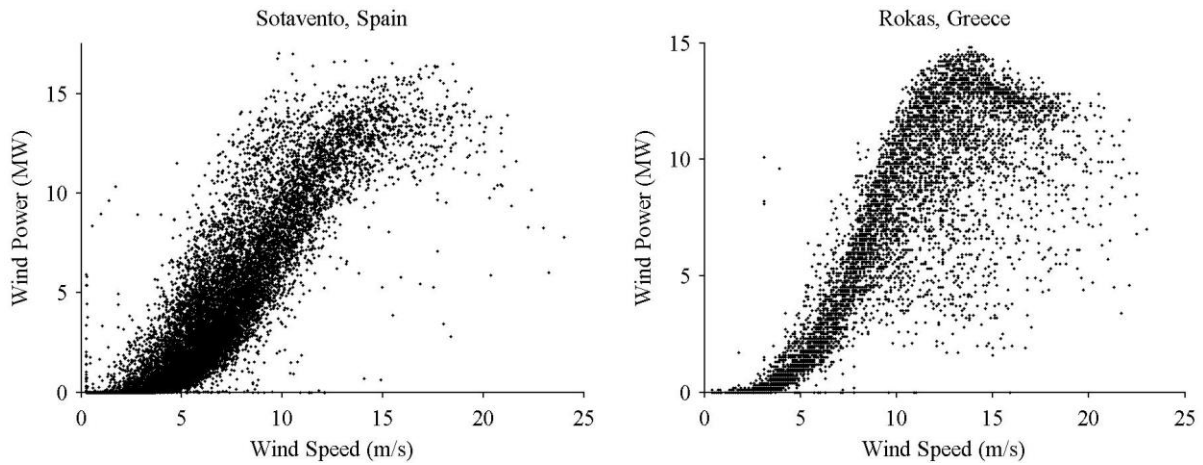
167
168
169 *2.2. Power curves*

170 The theoretical relationship between the wind power generated and the wind speed is
171 described by the machine power curve, which can be provided by the turbine manufacturer
172 [18]. This curve is deterministic and nonlinear, with the following features: a minimum
173 ‘connection speed’ below which no power can be generated; as speed rises from this
174 minimum, the power output increases; this continues until a ‘nominal speed’, which is the
175 lowest speed at which the turbine is producing at its maximum power output; and finally
176 there is a ‘disconnection speed’ at which the turbine must be shut down to avoid damage.

177 Fig. 3 plots the empirical power curves, using historical observations, for Sotavento
178 and Rokas. Although the figures show the essential features that we have just described for
179 the machine power curve, it can be seen that, in reality, the power curve for a wind farm is
180 stochastic. Sanchez [18] attributes this to the effect of other atmospheric variables, such as air
181 temperature and pressure, as well as other factors, such as the relationship differing for rising

182 and falling wind speed, complexities caused by the aggregated effect of different types of
183 turbines in the one wind farm, and the capacity of the wind farm varying over time.

184



185
186
187

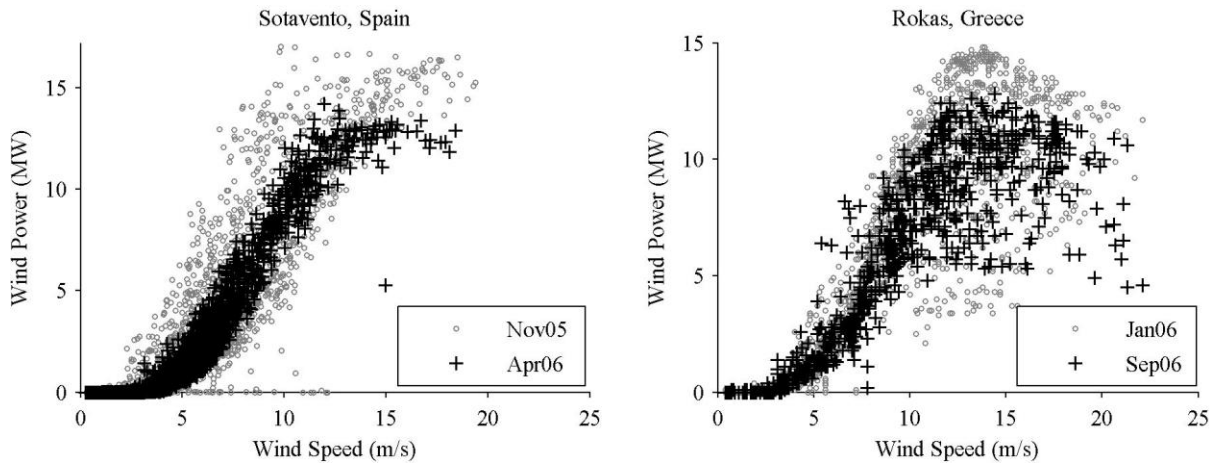
Fig. 3. Empirical power curves for Sotavento and Rokas.

188 The empirical power curves in Fig. 3 indicate that the dispersion and distributional
189 shape of the variability in wind power depends on the value of wind speed. For example, for
190 Rokas, if wind speed is between about 10 and 15 m/s, the wind power density is skewed to
191 the left with relatively high variability, while for wind speed below about 5 m/s, the wind
192 power density would seem to be skewed to the right with relatively low variability.
193 Therefore, the estimation of the wind power density or quantiles should be conditional on the
194 value of wind speed.

195 For Sotavento and Rokas, Fig. 4 shows the empirical power curves plotted for two
196 different months. The Sotavento plot shows considerably more variation in November 2005
197 than in April 2006. Curiously, for the higher values of wind speed, more wind power tended
198 to be generated in November 2005 than April 2006. A similar comment can be made
199 regarding the Rokas empirical power curve, which shows greater efficiency in the conversion
200 of strong values of wind speed to power in January 2006 than September 2006. In essence,
201 the plots suggest that the power curves are time-varying. This can be due to changing weather
202 patterns, and changes in the capacity of the wind farm due, for example, to maintenance or

203 expansion. Time-variation in the power curve suggests that, when modelling, it may be useful
204 to put more weight on more recent information.

205



206

207 **Fig. 4.** Empirical power curves for Sotavento and Rokas. Each based on two selected months.

208

209 The plots of this section indicate that, when forecasting wind power based on a model
210 relating power to speed, it is important to acknowledge two issues. First, the relationship
211 between wind power and speed is nonlinear and stochastic, and it may be time-varying and
212 dependent on wind direction and other atmospheric variables [18]. Second, the stochastic
213 nature of wind speed will affect the uncertainty in wind power predictions [19], and so should
214 be accommodated in the modelling approach. In the next section, we present a methodology
215 for wind power forecasting that addresses the first of these issues through the use of a
216 nonparametric approach that makes no distributional assumption for wind power, imposes no
217 parametric assumption for the relationship between wind power and speed, and puts more
218 weight on more recent observations. The methodology addresses the second issue by
219 incorporating Monte Carlo sampling from wind velocity density forecasts. These density
220 forecasts could be produced from a time series model or from weather ensemble predictions
221 from an atmospheric model.

222

223

224

225 3. Conditional kernel estimation for wind power density forecasting

226 3.1. Conditional kernel density estimation

227 Kernel density estimation is a nonparametric approach to the estimation of the density
228 of a target variable Y_t . It can be viewed as smoothing the empirical distribution of historical
229 observations. The unconditional kernel density (UKD) estimator (see [20]) is expressed as:

$$230 \quad \hat{f}(y) = \sum_{t=1}^n K_{h_y}(Y_t - y), \quad (1)$$

231 where n is the sample size, and $K_h(\bullet)=K(\bullet/h)/h$ is a kernel function with bandwidth h . The
232 kernel function is a function that integrates to 1. A common choice is the standard Gaussian
233 probability density function, and we use this for all kernel functions in this paper. The
234 bandwidth is a parameter that controls the degree of smoothing.

235 In its simplest form, conditional kernel density (CKD) estimation enables the
236 nonparametric estimation of the density of a target variable Y_t , conditional on the value of an
237 explanatory variable X_t . It is nonparametric in two senses: it requires no parametric
238 assumptions for either the distribution of Y_t or the form of the functional relationship between
239 Y_t and X_t . These features make the method particularly attractive for the wind power context,
240 because the wind power distribution is non-Gaussian and unknown, and the form of the
241 relationship between wind power and speed is nonlinear and unknown. The CKD estimator of
242 the conditional density function of Y_t , given $X_t = x$ (see [21]), is expressed as:

$$243 \quad \hat{f}(y | x) = \frac{\sum_{t=1}^n K_{h_x}(X_t - x) K_{h_y}(Y_t - y)}{\sum_{t=1}^n K_{h_x}(X_t - x)}.$$

244 The kernel K_{h_y} enables kernel density estimation in the y -axis direction, with the
245 observations weighted in accordance to the kernel K_{h_x} , which relates to kernel smoothing in
246 the x -axis direction, enabling a larger weight to be put on historical observations for which X_t
247 is closer to x . For the two kernels, the bandwidths, h_x and h_y , control the degree of smoothing.

248 3.2. Conditional kernel density estimation for wind power density forecasting

249 With wind power specified as the target variable Y_t , Jeon and Taylor [6] use CKD
 250 estimation with conditioning on wind velocity variables, U_t and V_t , which are the result of
 251 transforming wind speed and direction to Cartesian coordinates. They incorporate a decay
 252 parameter λ to enable more weight to be put on more recent observations. This is appealing
 253 because the shape of the wind power density, and its relationship to wind velocity, can vary
 254 over time. We noted this in Section 2.2, in relation to the two plots of Fig. 4, which each
 255 show the empirical power curve differing for two separate months of the year. A lower value
 256 of λ leads to faster decay. The CKD estimator is presented in the following expression:

$$257 \quad \hat{f}(y | u, v) = \frac{\sum_{t=1}^n \lambda^{n-t} K_{h_{uv}}(U_t - u) K_{h_{uv}}(V_t - v) K_{h_y}(Y_t - y)}{\sum_{t=1}^n \lambda^{n-t} K_{h_{uv}}(U_t - u) K_{h_{uv}}(V_t - v)} \quad (2)$$

258 Cross-validation can be used to optimise λ along with the bandwidths h_{uv} and h_y , and
 259 we discuss this issue further in the next section. The exponential decay can be viewed as a
 260 kernel function, defined to be one-sided with exponentially declining weight [22]. We can,
 261 therefore, view the CKD estimator of expression (2) as having three bandwidths, λ , h_{uv} and
 262 h_y . The CKD estimator provides an estimate of the density at $Y_t=y$. To estimate the full
 263 density, the CKD estimation can be performed for values of y from zero to the wind farm's
 264 capacity with small increments. In our implementations of CKD in this paper, we used
 265 increments equal to 1% of the capacity, and assumed equal probability within each of the
 266 corresponding 100 wind power intervals to deliver an estimate of the full density.

267 To produce a wind power density forecast, it seems natural to perform the CKD
 268 estimation conditional on forecasts of U_t and V_t . This is essentially the approach taken by
 269 Juban et al. [23], who condition on point forecasts of wind speed and direction from an
 270 atmospheric model. The problem with conditioning on point forecasts is that the resulting
 271 wind power density estimate will not capture the potentially significant uncertainty in U_t and

272 V_t . To address this, Jeon and Taylor [6] provide the following three-stage methodology that
273 effectively enables CKD estimation to be performed conditional on density forecasts for U_t
274 and V_t , which they produced using a time series model:

275 Stage 1 - The CKD estimator of expression (2) is used to produce an estimate of the full wind
276 power density conditional on each pair of values of U_t and V_t , on a grid from -30 m/s to 30
277 m/s with an increment of 0.5 m/s. The result is $121 \times 121 = 14,641$ pairs, and, for each, a
278 corresponding conditional wind power density estimate. These are stored for use in Stage 2.

279 Stage 2 - Monte Carlo simulation of a time series model is performed to deliver 1,000
280 realisations of pairs of values for U_t and V_t , for a selected lead time. Each value is rounded to
281 the nearest 0.5 m/s, and then for each of the 1,000 pairs, the corresponding conditional wind
282 power density estimate is obtained from those stored in Stage 1.

283 Stage 3 - The 1,000 wind power density estimates from Stage 2 are averaged to give a single
284 wind power density forecast.

285 It is worth noting that the methodology relies on density forecasts for the wind
286 velocities, U_t and V_t , and that these could be produced by a time series model or atmospheric
287 model, which would be expected to capture the autocorrelation properties of the wind.

288

289 *3.3. Optimising conditional kernel density estimation for wind power density forecasting*

290 Fan and Yim [24] and Hall et al. [25] provide support for the use of cross-validation
291 to optimise the bandwidths in kernel density estimation. In our implementation of kernel
292 density estimation in this paper, we followed Jeon and Taylor [6] by using a rolling window
293 of 6 months to produce density estimates, and by selecting the values of λ , h_{uv} and h_y that led
294 to the most accurate wind power density estimates calculated over a cross-validation
295 evaluation period for 1 hour-ahead prediction. They measured accuracy using the mean of the
296 continuous ranked probability score (CRPS), which is described by Gneiting et al. [26] as an

297 appealing measure of accuracy, capturing the properties of calibration and sharpness in the
298 estimate of the probability density function.

299 As we explained in the previous section, in our implementation of the kernel density
300 methods, we estimated the density for values of wind power at increments equal to 1% of the
301 capacity, and assumed equal probability within each of the 100 wind power intervals. As this
302 delivers a discrete density and distribution, we evaluated accuracy using the RPS, which is
303 the discrete version of the CRPS (see [27]).

304 We used a three-step cascaded optimisation approach to find the parameter values that
305 minimise the RPS for the cross-validation period. The first step involved a grid search of 100
306 values for λ , h_{uv} and h_y , log-equally spaced between the following intervals: $0.98 \leq \lambda \leq 1$;
307 $0.0001 \leq h_{uv} \leq 5$; and $0.001 \leq h_y \leq 0.5$. With regard to the interval for h_y , note that, instead of
308 working with wind power measured in MW, we used the capacity factor, which is wind
309 power as a proportion of the wind farm's capacity. The second step of the cascaded
310 optimisation approach used a trust-region-reflective algorithm, available in the 'fmincon'
311 function of Matlab® and described in [28]. The algorithm uses finite difference
312 approximations and trust regions to ensure the robustness of the iteration. A genetic algorithm
313 was chosen as the final step of the cascaded optimisation, with the best individuals from the
314 previous optimisations used as the population. We did not employ the genetic algorithm for
315 global optimisation (instead of our three-stage cascaded optimisation), because we found that
316 the genetic algorithm tended to find local optima. This problem has been recognised in the
317 use of genetic algorithms (see [29]), and although increasing the mutation rate or maintaining
318 a diverse population might help, this would be at the expense of an exponential increase in
319 the size of the search space. We use the notation CKD λ to refer to the three-stage CKD-based
320 approach of Section 3.2, optimised using the RPS.

321

322

323 **4. Conditional kernel estimation for wind power quantile forecasting**

324 In this section, we introduce our proposed approach to wind power quantile
325 forecasting. It is a relatively simple adaptation of the CKD approach of the previous section.

326

327 *4.1. A limitation of the CKD approach for wind power quantile forecasting*

328 Although CKD λ can certainly be used to deliver quantile forecasts, we would suggest
329 that this has the disadvantage that CKD λ involves the use of the same parameters across
330 different wind power quantiles. With regard to the bandwidth in the wind power direction, h_y ,
331 one might imagine that a larger value would be needed for more extreme quantiles, because
332 there are fewer observations in the tails of the density. With regard to the bandwidth in the
333 wind velocity directions, h_{uv} , it seems likely that the optimal value will depend on the value
334 of h_y , as well as the characteristics of the empirical power curve around the quantile under
335 consideration. For example, if that part of the empirical power curve has a relatively high
336 gradient, then a relatively small value of h_{uv} may be needed to avoid over-smoothing. As for
337 the decay parameter, λ , it seems reasonable to assume that different parts of the wind power
338 density will evolve at different rates, and also that the conditionality on the wind velocities
339 may evolve differently for different quantiles. Hence, different values of λ are likely to be
340 optimal for different quantiles. Therefore, the assumption of using the same parameters for
341 different quantiles would seem to hamper accurate quantile estimation.

342

343 *4.2. Optimising conditional kernel density estimation for wind power quantile forecasting*

344 In this paper, we use the three-stage CKD-based approach, described in Section 3.2,
345 to deliver a wind power density forecast, which we convert into a cumulative distribution
346 function from which we obtain the required θ quantile estimate. However, as our interest is
347 not in the accurate estimation of the entire wind power density, we optimise the approach

348 specifically towards estimation of the desired θ quantile of interest. More specifically, in the
 349 cross-validation approach used to optimise λ , h_{uv} and h_y , we replace the RPS with the
 350 following measure, which is the objective function minimised in quantile regression [30]:

$$351 \quad \frac{1}{n} \sum_{t=1}^n (Y_t - \hat{Q}_{y_t}) (\theta - I(Y_t \leq \hat{Q}_{y_t})) \quad (3)$$

352 where \hat{Q}_{y_t} is an estimate of the θ quantile of a variable Y_t . We refer to expression (3) as the
 353 mean quantile regression error (MQRE). It has been proposed as a measure of quantile
 354 forecast accuracy, both in the context of wind power [13,31] and in other applications
 355 [32,33,34]. We discuss this further in Section 5.3.

356 Our proposal is, therefore, to produce wind power quantile forecasts using the three-
 357 stage CKD-based approach of Section 3.2, with values of λ , h_{uv} and h_y selected to deliver the
 358 most accurate quantile estimates, where accuracy is measured using the MQRE, calculated
 359 over a cross-validation evaluation period for 1 hour-ahead prediction. We refer to this method
 360 as CKQ λ . In our empirical work, to minimise the MQRE for the cross-validation period, we
 361 used the three-step cascaded optimisation approach that we described in Section 3.3.

362

363 **5. Empirical study**

364 In this section, we use the hourly data from the three wind farms, described in Section
 365 2, to evaluate forecast accuracy for the 1%, 5%, 25%, 50%, 75%, 95%, and 99% conditional
 366 quantiles for lead times from 1 to 72 hours ahead. For each wind farm, we used the final 25%
 367 of data for post-sample evaluation, and the penultimate 25% for cross-validation.

368

369 *5.1. Kernel density methods for quantile forecasting*

370 In addition to the CKQ λ method, described in Section 4.2, we also implemented, as a
 371 sophisticated benchmark, the CKD λ method, described in Sections 3.2 and 3.3. These two

372 methods differ in that CKD λ uses the RPS as the basis for estimating the parameters, λ , h_{uv}
373 and h_y , while CKQ λ uses the quantile regression cost function of expression (3) for
374 estimation. For a given lead time, each of these methods delivers a wind power density
375 forecast, from which the required θ quantile forecast is obtained. We used a 6-month moving
376 window in the CKD estimation, with CKD estimation performed afresh every 24 hours.

377 Density forecasts of the wind velocity variables, U_t and V_t , were produced using a
378 time series model of the form used by Jeon and Taylor [6], with parameters estimated using
379 the first 75% of the data. This is a bivariate model with vector autoregressive moving average
380 components for the levels, and GARCH components for the variances. Interesting alternative
381 time series models for wind speed and direction include the multivariate kernel density
382 estimation approach of Zhang et al. [35], and the Bayesian approach of Jiang et al. [36].

383 As a relatively simple benchmark method, we applied the unconditional kernel
384 density (UKD) estimator of expression (1) to a moving window of the most recent historical
385 wind power observations. We optimised the one bandwidth using cross-validation. The
386 resulting density estimate provided quantile estimates that we used as the wind power
387 quantile forecasts for all future periods. We considered moving windows of lengths 24 hours,
388 10 days and 6 months. The best results were produced with moving windows of 24 hours, and
389 so for simplicity we report only these results in the remainder of this paper. We refer to this
390 method as UKD24.

391 Table 1 presents the parameters optimised for the three methods using cross-
392 validation, and averaged over the three wind farms. Note that the bandwidth in the y -
393 direction, h_y , has no units because, as we stated in Section 3.3, in our computations, we
394 worked with capacity factor, which is wind power as a proportion of the capacity of the wind
395 farm. In Table 1, each value of the decay parameter λ is accompanied by the corresponding
396 half-life, and these indicate that, although the values of λ may seem rather high, they do
397 imply notable decreasing weight over the 6-month rolling window of hourly observations

398 used for CKD λ and CKQ λ . For the CKQ λ method, it is interesting to note that the bandwidth
 399 in the y -direction, h_y , is larger for more extreme quantiles in the upper tail of the density. This
 400 bandwidth relates to kernel density estimation for the wind power density. The need for
 401 larger values of h_y for more extreme upper quantiles seems intuitive, because there are fewer
 402 observations in the upper tail of the wind power distribution, and hence more kernel
 403 smoothing is beneficial. With regard to the values of h_{uv} for CKQ λ , it is interesting to note
 404 that the values for the 1% quantile and 5% quantile, are notably larger than for the other
 405 quantiles. This implies a relatively large degree of smoothing of the empirical power curve,
 406 and this seems reasonable as the curve is relatively flat for low values of wind speed. Using a
 407 standard 64-bit (Intel i5, 1.6GHz) computer, our Matlab code took about two days to optimise
 408 each row of parameters in Table 1. However, this time could be reduced substantially by
 409 adjusting the details (such as genetic algorithm population size) of the three-step cascaded
 410 optimisation approach, described in Section 3.3, and by using multiple processors.

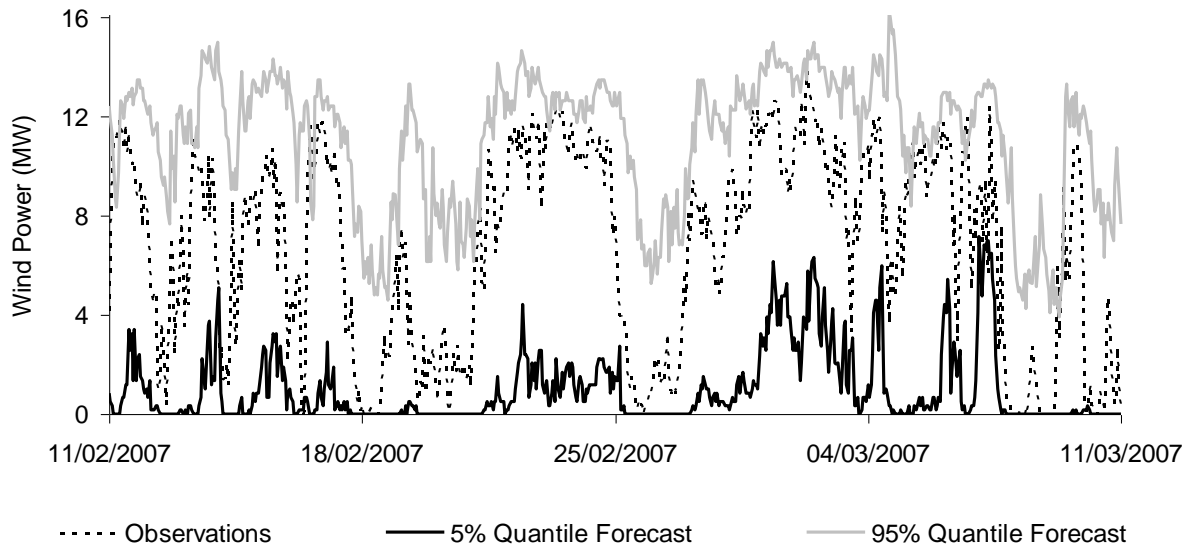
411 **Table 1**
 412 Parameters optimised using cross-validation for Sotavento.
 413
 414

Method	Bandwidth h_{uv} (m/s)	Bandwidth h_y	λ (half-life)
UKD24		0.267	
CKD λ	0.56	0.021	0.999 (28.9 days)
CKQ λ -1%	2.55	0.012	0.990 (2.9 days)
CKQ λ -5%	0.87	0.015	0.999 (28.9 days)
CKQ λ -25%	0.40	0.013	0.999 (28.9 days)
CKQ λ -50%	0.50	0.021	0.999 (28.9 days)
CKQ λ -75%	0.58	0.010	0.999 (28.9 days)
CKQ λ -95%	0.53	0.065	0.999 (28.9 days)
CKQ λ -99%	0.46	0.090	0.999 (28.9 days)

415
 416 NOTE: h_y has no units, because y is the capacity factor.
 417

418 In Fig. 5, we present the wind power observations and the 6 hour-ahead forecasts for
 419 the 5% and 95% quantiles from the CKQ λ method for the final 4 weeks of the post-sample
 420 period for Sotavento. It is reassuring to see that the quantile forecasts move with the wind

421 power time series. However, the purpose of Fig. 5 is to provide just an informal visual check
 422 on the method. A more thorough assessment of quantile forecast accuracy is provided in
 423 Section 5.3.



424 **Fig. 5.** Time series plots of 6 hour-ahead quantile forecasts from CKQ λ for the final 4 weeks
 425 of the post-sample period for Sotavento.
 426
 427

428 5.2. A quantile regression method for quantile forecasting

429 In addition to the methods, described in the previous section, we generated quantile
 430 forecasts from a quantile regression modelling approach, based on the work of Nielsen et al.
 431 [14]. This involves first producing point forecasts, and then using quantile regression to
 432 estimate quantile models for the forecast error. For simplicity, as point forecasts, we used the
 433 median of the density forecasts of the UKD24 method, which we described in Section 5.1.

434 Following the approach taken by Nielsen et al., we chose the quantile regression
 435 dependent variable to be a vector constructed by concatenating vectors of $(n-72)$ in-sample
 436 forecast errors for each of the 72 lead times of interest, where n is the number of in-sample
 437 periods. We included an intercept (C) in the quantile regression, and the following
 438 explanatory variables: the lead time (L); the square of the lead time (L^2); the value of the
 439 wind power capacity factor at the forecast origin (P); the value of the capacity factor at the
 440 forecast origin multiplied by the lead time ($P \times L$); the value of the capacity factor at the

441 forecast origin multiplied by the square of the lead time ($P \times L^2$); the value of wind speed at
 442 the forecast origin (S); the value of wind speed at the forecast origin multiplied by the lead
 443 time ($S \times L$); the value of wind speed at the forecast origin multiplied by the square of the lead
 444 time ($S \times L^2$); and the point forecast for wind power (\hat{P}).

445 We performed the quantile regression for each of the seven probability levels (1%,
 446 5%, 25%, 50%, 75%, 95%, and 99%), and for each wind farm. This delivered forecast error
 447 quantiles. Each wind power quantile forecast was then produced as the sum of the point
 448 forecast and the forecast error quantile. A sizeable number of the resulting wind power
 449 quantile forecasts were less than zero or greater than the wind farm's capacity. When this
 450 occurred, we adjusted the forecast, so that it fell within this interval. Table 2 provides the
 451 parameters estimated for the 5% and 95% quantile regression models for Sotavento. Given
 452 that L takes values up to 72, the coefficients of L^2 , $P \times L$ and $P \times L^2$ are sufficiently large to
 453 imply that the wind power uncertainty is nonlinearly dependent on the lead time and wind
 454 power capacity factor at the forecast origin.

455 **Table 2**
 456 Parameters of the 5% and 95% quantile regression models for Sotavento.

	C	L	L^2	P	$P \times L$	$P \times L^2$	S	$S \times L$	$S \times L^2$	\hat{P}
5%	0.0254	-0.054	-0.00072	1.56	0.0024	-0.00074	-0.0176	0.00200	0.000045	-7.56
95%	0.0161	0.026	-0.00025	1.79	-0.0477	0.00026	-0.0180	0.00008	0.000006	-0.92

458

459 5.3. Comparison of post-sample quantile forecast accuracy

460 In the context of probabilistic wind power forecasting, Pinson et al. [31] describe how
 461 quantile forecasts should be assessed in terms of *reliability* and *sharpness*. Reliability is the
 462 degree to which the quantile forecast is, on average, correct. Sharpness, which is also
 463 sometimes called *resolution*, is the extent to which the quantile forecast varies with the
 464 quantile over time. To assess the post-sample performance of the wind power quantile
 465 forecasting methods, we used two measures: the hit percentage and the MQRE of expression

466 (3). The hit percentage, that we consider here, is a standard measure of reliability (see, e.g.,
467 [31] and [37]). Pinson et al. [31] explain that, having assessed reliability, sharpness can be
468 evaluated through the use of the MQRE, which is an overall skill score, measuring both
469 reliability and sharpness.

470 The hit percentage is the percentage of the post-sample wind power observations that
471 fall below the corresponding quantile forecasts. For estimation of the θ quantile, the ideal
472 value for the hit percentage is θ . For each method and forecast lead time, we calculated the
473 weighted average of the hit percentage across the three wind farms, where the weights were
474 in proportion to the capacities of the wind farms. We present this average hit percentage in
475 Table 3. For clarity of presentation, in Table 3, we group some of the forecast horizons
476 together, with more detailed results shown for the early lead times, as we feel all of the
477 methods have greatest potential for shorter lead times, as they are based in this paper on time
478 series models, rather than on predictions from an atmospheric model. The final column of the
479 table provides the average performance across all lead times. Table 3 shows the simple
480 benchmark method, UKD24, performing relatively poorly, except for estimation of the 75%
481 quantiles. Looking at the final column of Table 3, we see that, overall, CKQ λ performed the
482 best for four of the seven quantile probability levels, and was poorer than CKD λ for just the
483 25% and 50% probability levels. The quantile regression method was relatively poor for the
484 lower three probability levels, but the best overall for estimation of the 95% quantiles, and
485 competitive for estimation of the 75% and 99% quantiles.

486 The hit percentage is a measure of the unconditional coverage of a quantile estimator.
487 It assesses the average number of times that an observation falls below the estimator. To also
488 assess the degree to which each quantile estimator varies with the wind power series, tests
489 have been proposed for conditional coverage (e.g. [38]). These tests focus on the level of
490 autocorrelation in the series of hits. Unfortunately, these tests are not of use for multi-step-
491 ahead prediction, because the hit variable will naturally tend to be autocorrelated, regardless

492 of the quality of the quantile forecasts [31]. To assess both conditional and unconditional
493 coverage, we use the MQRE, presented in expression (3). As we discussed at the start of this
494 section, the MQRE can also be viewed as an overall skill score measuring both reliability and
495 sharpness. Its use for evaluating quantile forecasts is natural, in view of the common use of
496 the mean squared error (MSE) for evaluating point forecasts. Table 4 presents the weighted
497 average of the MQRE across the three wind farms, where the weighting was in proportion to
498 the capacities of the wind farms. In this table, the results for the UKD24 method are not
499 competitive for any of the quantiles. The results for the two conditional kernel methods are
500 the same for the lower three probability levels. For the other quantiles, $CKQ\lambda$ was more
501 accurate than $CKD\lambda$, but the results are quite similar for the three upper quantiles. For the
502 75% probability level, the results for the quantile regression approach are notably the best;
503 for the 50% probability level, this method was relatively poor; and for the other five
504 probability levels, the results for this approach are similar to those for the two conditional
505 kernel methods.

506 It is interesting to note that the hit percentage measure of Table 3 does not, in general,
507 noticeably deteriorate as the lead time increases. However, with regard to the MQRE in Table
508 4, this is only the case for the 1% and 5% probability levels. Therefore, we can conclude from
509 Tables 3 and 4 that, for the other five probability levels, although reliability remains
510 relatively stable as the lead time increases, the sharpness of the quantile forecasts becomes
511 poorer.

512 Table 5 investigates how the relative performances of the methods differ across the
513 three wind farms. For each wind farm, the table presents each of the two measures, averaged
514 across the 72 lead times, for each method. The results are reasonably consistent across the
515 three wind farms. An exception to this is that the $CKD\lambda$ method performed relatively poorly
516 for Aeolos. Another exception is that the UKD24 benchmark method was relatively accurate
517 for Sotavento for 95% and 99% quantile estimation.

518 **Table 3**
519 Evaluation of post-sample quantile forecasts using the hit percentage measure of reliability,
520 averaged over the three wind farms with weights in proportion to their capacities.
521

Horizon (hours)	1	2	3-4	5-6	7-8	9-12	13-24	25-48	49-60	61-72	1-72
1%											
UKD24	22.4	22.5	22.4	22.6	22.6	22.8	22.9	23.6	23.9	24.1	23.5
QuReg	0.2	0.1	0.0	<u>0.0</u>	<u>0.0</u>	0.0	0.0	0.0	<u>0.0</u>	<u>0.0</u>	0.0
CKD λ	<u>0.5</u>	<u>0.2</u>	<u>0.1</u>	<u>0.0</u>	<u>0.0</u>	<u>0.1</u>	0.1	0.1	<u>0.0</u>	<u>0.0</u>	0.0
CKQ λ	0.3	<u>0.2</u>	<u>0.1</u>	<u>0.0</u>	<u>0.0</u>	<u>0.1</u>	<u>0.2</u>	<u>0.2</u>	<u>0.0</u>	<u>0.0</u>	<u>0.1</u>
5%											
UKD24	28.1	28.2	28.2	28.5	28.7	28.8	28.8	29.7	30.2	30.8	29.6
QuReg	0.4	0.1	0.0	0.0	0.0	0.0	0.0	0.0	0.0	0.0	0.0
CKD λ	<u>1.6</u>	<u>1.3</u>	<u>1.3</u>	<u>1.4</u>	1.5	<u>1.6</u>	1.9	2.6	2.9	3.0	2.4
CKQ λ	1.5	<u>1.3</u>	1.2	1.3	<u>1.6</u>	<u>1.6</u>	<u>2.1</u>	<u>3.4</u>	<u>4.1</u>	<u>4.6</u>	<u>3.2</u>
25%											
UKD24	53.8	53.8	53.8	54.0	54.2	54.0	54.1	54.9	54.4	53.6	54.3
QuReg	<u>25.6</u>	19.8	15.3	11.9	9.2	5.9	1.7	1.0	1.1	1.9	3.1
CKD λ	18.1	19.4	20.5	21.6	22.6	<u>23.6</u>	<u>23.4</u>	<u>22.1</u>	<u>21.2</u>	<u>20.3</u>	<u>21.8</u>
CKQ λ	22.1	<u>23.6</u>	<u>24.9</u>	<u>26.1</u>	<u>26.7</u>	28.3	30.4	30.2	30.3	30.2	29.6
50%											
UKD24	68.9	69.0	68.8	68.8	68.6	68.5	68.2	67.9	67.5	66.6	67.8
QuReg	44.3	46.5	47.9	49.5	51.1	52.6	55.3	60.6	62.8	63.5	58.8
CKD λ	53.2	53.0	<u>51.6</u>	<u>50.4</u>	<u>49.7</u>	<u>48.5</u>	<u>46.9</u>	<u>45.8</u>	<u>44.6</u>	<u>44.3</u>	<u>46.3</u>
CKQ λ	<u>50.4</u>	<u>49.7</u>	<u>48.4</u>	47.3	46.7	45.8	45.0	44.5	43.9	43.6	44.8
75%											
UKD24	82.8	82.4	82.3	81.9	81.5	81.3	80.8	79.3	<u>78.5</u>	<u>77.4</u>	79.5
QuReg	81.4	78.3	76.2	<u>75.0</u>	74.9	75.3	77.0	78.4	78.9	78.4	77.9
CKD λ	<u>79.5</u>	<u>77.4</u>	<u>75.9</u>	74.5	73.8	73.0	70.8	68.1	66.3	65.5	68.9
CKQ λ	<u>79.5</u>	77.7	76.4	75.3	<u>75.0</u>	<u>74.8</u>	<u>73.6</u>	<u>71.9</u>	71.0	70.6	<u>72.5</u>
95%											
UKD24	92.6	92.2	92.0	91.9	91.6	91.5	91.4	90.5	89.6	89.0	90.5
QuReg	87.8	90.0	90.3	90.2	90.5	91.1	93.7	97.3	97.5	<u>95.0</u>	<u>95.2</u>
CKD λ	<u>96.6</u>	<u>96.0</u>	<u>95.8</u>	<u>95.3</u>	<u>94.6</u>	<u>94.2</u>	93.4	92.1	91.1	90.6	92.4
CKQ λ	97.7	97.5	97.2	97.1	96.8	96.6	<u>96.2</u>	<u>95.4</u>	<u>94.7</u>	94.5	95.5
99%											
UKD24	96.5	96.4	96.2	96.0	95.8	95.9	95.8	95.3	94.7	94.4	95.2
QuReg	96.4	96.2	95.9	96.3	96.4	96.6	97.8	99.3	99.7	98.8	98.5
CKD λ	<u>99.0</u>	<u>99.0</u>	<u>99.1</u>	<u>99.2</u>	<u>99.0</u>	<u>98.9</u>	98.7	98.0	97.6	97.5	98.1
CKQ λ	99.4	99.3	99.4	99.5	99.4	99.3	<u>99.2</u>	<u>98.9</u>	<u>98.9</u>	<u>98.9</u>	<u>99.0</u>

522
523 NOTE: For the θ quantile, the ideal value is θ . The best performing method at each horizon is underlined.
524
525
526
527
528

529 **Table 4**
530 Evaluation of post-sample quantile forecasts using the MQRE ($\times 1,000$) skill score (measuring
531 both reliability and sharpness), averaged over the three wind farms with weights in proportion
532 to their capacities.
533

Horizon (hours)	1	2	3-4	5-6	7-8	9-12	13-24	25-48	49-60	61-72	1-72
1%											
UKD24	8	8	8	9	9	9	10	12	13	14	12
QuReg	<u>3</u>	<u>3</u>	<u>3</u>								
CKD λ	3	<u>3</u>	<u>3</u>	<u>3</u>							
CKQ λ	3	<u>3</u>	<u>3</u>	<u>3</u>							
5%											
UKD24	28	28	28	29	30	31	32	35	38	39	35
QuReg	13	13	13	13	13	<u>13</u>	<u>13</u>	<u>13</u>	<u>13</u>	<u>13</u>	<u>13</u>
CKD λ	<u>10</u>	<u>11</u>	<u>12</u>	<u>12</u>	<u>12</u>	<u>13</u>	<u>13</u>	<u>13</u>	<u>13</u>	14	<u>13</u>
CKQ λ	11	<u>11</u>	<u>12</u>	<u>12</u>	13	<u>13</u>	<u>13</u>	14	14	14	<u>13</u>
25%											
UKD24	92	93	94	95	96	98	99	104	108	111	104
QuReg	<u>23</u>	<u>32</u>	<u>41</u>	49	55	60	65	67	69	71	64
CKD λ	35	39	43	<u>47</u>	51	<u>55</u>	<u>61</u>	<u>66</u>	<u>67</u>	<u>67</u>	<u>63</u>
CKQ λ	34	38	42	<u>47</u>	<u>50</u>	<u>55</u>	<u>61</u>	67	68	68	<u>63</u>
50%											
UKD24	119	120	122	124	125	126	127	133	137	140	132
QuReg	65	70	75	81	86	90	100	115	129	136	113
CKD λ	44	51	60	68	75	83	97	113	120	121	105
CKQ λ	<u>40</u>	<u>46</u>	<u>52</u>	<u>59</u>	<u>65</u>	<u>71</u>	<u>83</u>	<u>97</u>	<u>104</u>	<u>106</u>	<u>91</u>
75%											
UKD24	100	100	102	103	104	105	106	110	114	116	110
QuReg	<u>28</u>	<u>38</u>	<u>48</u>	<u>58</u>	<u>65</u>	<u>72</u>	<u>82</u>	<u>98</u>	<u>104</u>	<u>104</u>	<u>91</u>
CKD λ	36	44	51	60	67	76	92	111	122	124	104
CKQ λ	36	44	51	59	<u>65</u>	74	90	109	119	121	101
95%											
UKD24	36	37	37	38	39	39	39	40	42	43	40
QuReg	<u>13</u>	<u>16</u>	20	22	25	26	<u>27</u>	<u>29</u>	<u>30</u>	<u>29</u>	<u>28</u>
CKD λ	14	<u>16</u>	<u>18</u>	<u>21</u>	23	26	29	34	37	39	33
CKQ λ	15	17	19	<u>21</u>	<u>22</u>	<u>24</u>	<u>27</u>	<u>29</u>	<u>30</u>	30	<u>28</u>
99%											
UKD24	11	11	12	12	12	12	12	13	14	14	13
QuReg	6	6	7	7	8	8	7	<u>7</u>	<u>7</u>	8	7
CKD λ	<u>4</u>	<u>5</u>	<u>5</u>	<u>5</u>	<u>6</u>	<u>6</u>	7	<u>7</u>	<u>7</u>	<u>7</u>	7
CKQ λ	<u>4</u>	<u>5</u>	<u>5</u>	<u>5</u>	<u>6</u>	<u>6</u>	<u>6</u>	<u>7</u>	<u>7</u>	<u>7</u>	<u>6</u>

534 NOTE: Smaller values are better. The best performing method at each horizon is underlined.
535

536
537

538

539
540
541
542
543
544

Table 5
Evaluation of post-sample quantile forecasts using the hit percentage reliability measure and the MQRE ($\times 1,000$) skill score (measuring both reliability and sharpness). Values shown are averages across the 72 lead times. The weighted averages use weights in proportion to the capacities of the wind farms.

	Hit percentage				MQRE ($\times 1,000$)			
	Aeolos	Rokas	Sotavento	Wtd. Avg.	Aeolos	Rokas	Sotavento	Wtd. Avg.
1%								
UKD24	29.6	22.1	18.7	23.5	17	13	5	12
QuReg	<u>0.0</u>	0.0	<u>0.0</u>	0.0	<u>3</u>	<u>3</u>	<u>2</u>	<u>3</u>
CKD λ	<u>0.0</u>	0.1	<u>0.0</u>	0.0	<u>3</u>	<u>3</u>	<u>2</u>	<u>3</u>
CKQ λ	<u>0.0</u>	<u>0.3</u>	<u>0.0</u>	<u>0.1</u>	<u>3</u>	<u>3</u>	<u>2</u>	<u>3</u>
5%								
UKD24	35.4	28.9	24.7	29.6	47	39	18	35
QuReg	0.0	0.0	0.0	0.0	<u>14</u>	<u>14</u>	<u>11</u>	<u>13</u>
CKD λ	<u>0.1</u>	<u>7.0</u>	<u>0.2</u>	2.4	<u>14</u>	<u>14</u>	<u>11</u>	<u>13</u>
CKQ λ	<u>0.1</u>	9.1	<u>0.2</u>	<u>3.2</u>	<u>14</u>	<u>14</u>	<u>11</u>	<u>13</u>
25%								
UKD24	57.2	52.3	53.5	54.3	129	106	76	104
QuReg	2.1	5.6	1.6	3.1	69	70	54	64
CKD λ	7.1	<u>36.4</u>	21.7	<u>21.8</u>	<u>68</u>	<u>67</u>	<u>52</u>	<u>63</u>
CKQ λ	<u>30.1</u>	36.7	<u>22.0</u>	29.6	69	<u>67</u>	<u>52</u>	<u>63</u>
50%								
UKD24	67.1	66.1	70.2	67.8	159	131	107	132
QuReg	<u>50.0</u>	65.2	61.2	58.8	<u>80</u>	120	139	113
CKD λ	35.7	<u>59.0</u>	<u>44.1</u>	<u>46.3</u>	126	<u>107</u>	83	105
CKQ λ	38.5	61.9	34.1	44.8	123	109	<u>40</u>	<u>91</u>
75%								
UKD24	<u>78.3</u>	<u>76.9</u>	83.4	79.5	130	107	91	110
QuReg	79.8	81.9	71.8	77.9	<u>107</u>	94	<u>71</u>	<u>91</u>
CKD λ	54.3	80.5	<u>72.0</u>	68.9	143	<u>92</u>	76	104
CKQ λ	56.8	81.2	78.3	<u>72.5</u>	136	93	75	101
95%								
UKD24	89.1	88.0	94.3	90.5	48	43	29	40
QuReg	<u>96.5</u>	94.2	<u>94.9</u>	<u>95.2</u>	31	<u>28</u>	<u>24</u>	<u>28</u>
CKD λ	85.4	95.3	96.5	92.4	46	<u>28</u>	<u>24</u>	33
CKQ λ	93.0	<u>95.2</u>	98.3	95.5	<u>30</u>	<u>28</u>	25	<u>28</u>
99%								
UKD24	94.1	92.4	99.2	95.2	16	16	7	13
QuReg	<u>99.0</u>	97.6	<u>98.9</u>	98.5	7	8	7	7
CKD λ	96.3	<u>98.5</u>	99.6	98.1	8	<u>6</u>	<u>6</u>	7
CKQ λ	99.1	98.2	99.9	<u>99.0</u>	<u>6</u>	<u>6</u>	<u>6</u>	<u>6</u>

545
546
547

NOTE: For the θ quantile, the ideal value is θ . The best performing method in each column is underlined.

548 **6. Summary and concluding comments**

549 In many parts of the world, the move towards more sustainable power generation has
550 led to a rapid increase in installed wind power capacity. The assessment of the uncertainty in
551 the future power output from a wind farm is of great importance for the efficient management
552 of power systems and wind power plants. The accuracy of the forecasts of a specific quantile
553 of the wind power density is often of more relevance than the overall accuracy of an estimate
554 of the full density. For example, when wind power producers are offering power to the
555 market for a future period, the optimal bid is a quantile of the wind power density.

556 This paper has focused on a previously proposed CKD-based approach to wind power
557 density forecasting, which captures the uncertainty in wind velocity, and the uncertainty in
558 the power curve. It is appealing because it involves a nonparametric approach that makes no
559 distributional assumption for wind power, it imposes no parametric assumption for the
560 relationship between wind power and wind velocity, and it allows more weight to be put on
561 more recent observations. As we do not require an accurate estimate of the entire wind power
562 density, our new proposal in this paper is to optimise the CKD-based approach specifically
563 towards estimation of the desired quantile, using the quantile regression objective function.

564 Using data from three wind farms, we found that overall this approach delivered more
565 accurate quantile predictions than quantile forecasts derived from the density forecasts
566 produced by the original CKD-based method and by an unconditional kernel density
567 estimator. We also implemented a method, based on the work of Nielsen et al. [14], who
568 construct a wind power quantile as the sum of a point forecast and a forecast error quantile
569 estimated using quantile regression. Interestingly, the results of this method were competitive
570 with the conditional kernel approaches, especially in terms of the MQRE skill score. A
571 disadvantage of the quantile regression approach is that it is not clear how to constrain the
572 wind power quantile to be between zero and the capacity of the wind farm. Furthermore, we

573 suspect that quantile crossing (see Section 2.5 of [30]) will be more likely from a pair of
574 quantile regression models than from a CKD-based approach.

575 In future work, it would be interesting to evaluate empirically the conditional kernel
576 methods for wind velocity density forecasts based on weather ensemble predictions. It would
577 also be interesting to consider the possible incorporation of a copula in the CKD-based
578 approach, which would provide a representation of the interdependency between wind power
579 and the wind velocities (see [39]).

580

581 **Acknowledgements**

582 We are grateful to the Sotavento Galacia Foundation for making the Sotavento wind
583 farm data available. We would also like to thank George Sideratos of the National Technical
584 University of Athens and the EU SafeWind Project for providing the Greek wind farm data.
585 We are also grateful to three anonymous referees and an associate editor for their useful
586 comments on the paper.

587

588 **References**

- 589 [1] W. Katzenstein, E. Fertig, J. Apt, The variability of interconnected wind plants, *Energy Policy*. 38
590 (2010) 4400-4410.
- 591 [2] Y. Zhang, J. Wang, X. Wang, Review on probabilistic forecasting of wind power generation,
592 *Renewable and Sustainable Energy Reviews*. 32 (2014) 255-270.
- 593 [3] P. Pinson, C. Chevallier, G.N. Kariniotakis, Trading wind generation from short-term probabilistic
594 forecasts of wind power, *IEEE Transactions on Power Systems*. 22 (2007) 1148-1156.
- 595 [4] Y. Wang, Y. Xia, X. Liu, Establishing robust short-term distributions of load extremes of offshore
596 wind turbines, *Renewable Energy*. 57 (2013) 606-619.
- 597 [5] E. Cripps, W.T.M. Dunsmuir, Modelling the variability of Sydney Harbour wind measurements,
598 *Journal of Applied Meteorology*, 42 (2003) 1131-1138.
- 599 [6] J. Jeon, J.W. Taylor, Using conditional kernel density estimation for wind power forecasting, *Journal*
600 *of the American Statistical Association*. 107 (2012) 66-79.

- 601 [7] A.M. Foley, P.G. Leahy, A. Marvuglia, E.J. McKeogh, Current methods and advances in forecasting of
602 wind power generation, *Renewable Energy*. 37 (2012) 1-8.
- 603 [8] M.S. Roulston, D.T. Kaplan, J. Hardenberg, L.A. Smith, Using medium-range weather forecasts to
604 improve the value of wind energy production, *Renewable Energy*. 28 (2003) 585-602.
- 605 [9] J.W. Taylor, P.E. McSharry, R. Buizza, Wind power density forecasting using wind ensemble
606 predictions and time series models, *IEEE Transactions on Energy Conversion*. 24 (2009) 775-782.
- 607 [10] J.M. Sloughter, T. Gneiting, A.E. Raftery, Probabilistic wind speed forecasting using ensembles and
608 Bayesian model averaging, *Journal of the American Statistical Association*. 105 (2010) 25-35.
- 609 [11] M. Yoder, A.S. Hering, W.C. Navidi, K. Larson, Short-term forecasting of categorical changes in wind
610 power with Markov Chain models, *Wind Energy*. 17 (2014), 1425-1439.
- 611 [12] J.B. Bremnes, A comparison of a few statistical models for making quantile wind power forecasts,
612 *Wind Energy*. 9 (2006) 3-11.
- 613 [13] J.L. Møller, H.A. Nielsen, H. Madsen, Time-adaptive quantile regression, *Computational Statistics and
614 Data Analysis*. 52 (2008) 1292-1303.
- 615 [14] H.A. Nielsen, H. Madsen, T.S. Nielsen, Using quantile regression to extend an existing wind power
616 forecasting system with probabilistic forecasts, *Wind Energy*. 9 (2006) 95-108.
- 617 [15] J.W. Taylor, D.W. Bunn, A quantile regression approach to generating prediction intervals,
618 *Management Science*. 45 (1999) 225-237.
- 619 [16] A. Bossavy, R. Girard, G. Kariniotakis, Forecasting ramps of wind power production with numerical
620 weather prediction ensembles, *Wind Energy*. 16 (2013) 51-63.
- 621 [17] R.S.J. Tol, Autoregressive conditional heteroscedasticity in daily wind speed measurements.
622 *Theoretical Applied Climatology*. 56 (1997) 113-122.
- 623 [18] I. Sanchez, Short-term prediction of wind energy production, *International Journal of Forecasting*. 22
624 (2006) 43-56.
- 625 [19] A.S. Hering, M.G. Genton, Powering up with space-time wind forecasting, *Journal of the American
626 Statistical Association*. 105 (2010) 92-104.
- 627 [20] B.W. Silverman, *Density Estimation for Statistics and Data Analysis*, Chapman and Hall, London,
628 1986.
- 629 [21] M. Rosenblatt, Conditional probability density and regression estimators, in: P.R. Krishnaiah (Ed.),
630 *Multivariate Analysis II*, Academic Press, New York, 1969, pp. 25-31.

- 631 [22] I. Gijbels, A. Pope, M.P. Wand, Understanding exponential smoothing via kernel regression, *Journal of the*
632 *Royal Statistical Society Series B.* 61 (1999) 39-50.
- 633 [23] J. Juban, L. Fugon, G. Kariniotakis, Probabilistic short-term wind power forecasting based on kernel
634 density estimators, *European Wind Energy Conference, Milan, Italy, 2007.*
- 635 [24] J. Fan, T.H. Yim, A crossvalidation method for estimating conditional densities, *Biometrika.* 91 (2004)
636 819-834.
- 637 [25] P. Hall, J. Racine, Q. Li, Cross-validation and the estimation of conditional probability densities,
638 *Journal of the American Statistical Association.* 99 (2004) 1015-1026.
- 639 [26] T. Gneiting, F. Balabdaoui, A.E. Raftery, Probabilistic forecasts, calibration and sharpness, *Journal of*
640 *the Royal Statistical Society. Series B: Statistical Methodology.* 69 (2007) 243-268.
- 641 [27] E.S. Epstein, A scoring system for probability forecasts of ranked categories, *Journal of Applied*
642 *Meteorology.* 8 (1969) 985-987
- 643 [28] T.F. Coleman, Y. Li, An interior trust region approach for nonlinear minimization subject to bounds,
644 *SIAM Journal on Optimization.* 6 (1996) 418-445.
- 645 [29] D. E. Goldberg, Simple genetic algorithm and the minimal deceptive problem, pp 74-88, in L.D. Davis
646 (editor), *Genetic Algorithms and Simulated Annealing*, Morgan Kaufmann, San Mateo, CA, 1987.
- 647 [30] R.W. Koenker, *Quantile Regression*, Cambridge University Press, Cambridge, UK, 2005.
- 648 [31] P. Pinson, H.A. Nielsen, J.K. Moller, H. Madsen, G.N. Kariniotakis. Non-parametric probabilistic
649 forecasts of wind power: Required properties and evaluation. *Wind Energy.* 10 (2007) 497-516.
- 650 [32] R. Koenker, J.A.F. Machado. Goodness of fit and related inference processes for quantile regression.
651 *Journal of the American Statistical Association.* 94 (1999) 1296-1310.
- 652 [33] J.W. Taylor. Evaluating volatility and interval forecasts. *Journal of Forecasting* 18 (1999) 111-128.
- 653 [34] R. Giacomini, I. Komunjer. Evaluation and combination of conditional quantile forecasts. *Journal of*
654 *Business and Economic Statistics.* 23 (2005) 416-431.
- 655 [35] J. Zhang, S. Chowdhurya, A. Messac, L. Castillo, A multivariate and multimodal wind distribution
656 model, *Renewable Energy.* 51 (2013) 436-447.
- 657 [36] Y. Jiang, Z. Song, A. Kusiak, Very short-term wind speed forecasting with Bayesian structural break
658 model, *Renewable Energy.* 50 (2013) 637-647.
- 659 [37] P. Pinson, G.N. Kariniotakis. Conditional prediction intervals. *IEEE Transactions on Power Systems.*
660 25 (2010) 1845-1856.

- 661 [38] R.F. Engle, S. Manganelli, CAViaR: Conditional autoregressive value at risk by regression quantiles,
662 Journal of Business and Economic Statistics. 22 (2004) 367-382.
- 663 [39] R.J. Bessa, V. Miranda, A. Botterud, Z. Zhou, J. Wang, Time-adaptive quantile-copula for wind power
664 probabilistic forecasting, Renewable Energy. 40 (2012) 29-39.